View metadata, citation and similar papers at core.ac.uk
brought to you by CORE
provided by PolyU Institutional Repository

JOURNAL OF APPLIED PHYSICS VOLUME 93, NUMBER 12 15 JUNE 2003

Probing local electric field distribution of nanotube arrays using electrostatic force microscopy

Long Ba,[a] Jian Shu, and Zuhong Lu
Laboratory of Molecular and Biomolecular Electronics, Southeast University, Nanjing, 210096, China

Juntao Li, Wei Lei, and Baoping Wang
Department of Electronic Engineering, Southeast University, Nanjing, 210096, China

Waisang Li
Department of Electronic and Information Engineering, Hong Kong Polytechnic University, Hung Hum, Hong Kong SAR

(Received 23 July 2002; accepted 13 March 2003)

The local electric field distribution of nanotube arrays has been studied by using the electrostatic force microscopy (EFM) technique. The nanotube arrays were fabricated using the anodic alumina template method. Good electric contact has been proofed using contact mode conductive atomic force microscopy. The experiment shows that the EFM can provide a quantitative mapping tool to measure three-dimensional distribution of local electric field with resolution down to several nanometers. The finite difference method has been applied to calculate the electric field distribution near the surface of the nanotube array induced by a conductive tip. The results show that the field decays in a power law with exponent varies for nanotubes of different packing environments as the tip was lifted away from the top of nanotubes. The protrusion of nanotubes causes a much higher enhanced field than packing geometry. Medium packing density may enable the maximum collective emission current for such nanotube arrays of narrow diameter and height diversity.
© *2003 American Institute of Physics.* [DOI: 10.1063/1.1571963]

I. INTRODUCTION

The unique field emission properties of the carbon nanotube have been extensively studied in the last years.[1–3] Its relative low electron escaping work,[3,4] very sharp tip curvature of several nanometers, and very stable structure under high electric field[5] enable it to be a very promising material of the electron emission source. For a high quality field emission display device, it is critical to provide a good electron emitter that has enough lateral uniformity and time endurance. Especially in the case of a gated structure, the flat top topography of a vertical nanotube film and even distribution of the lateral distribution will be more essential, because less fluctuation of the electron emission among thousands of pixel cells of a display area would cause higher brightness fluctuation.

Though the understanding to the local electric field within a nanometer scale is important for the design of practical field emission devices, it is quite difficult to implement quantitative measurement to this field distribution. The electrostatic force microscopy (EFM) is a useful tool to give three-dimensional (3D) mapping of the electric field gradient as well as surface topography.[6] By using a conductive tip as a nanosize probe, the space field above the sample surface can be measured from the quantitative electrostatic force sensed by the cantilever. In this article, we will present our experimental and numerical studies on the local electric field at the surface of the nanotube thin film induced by a conductive tip. The local electric field is transformed from the force gradient measured above the nanotube arrays, which has been fabricated using the anodic alumina template method. By assuming the nanotube as a nanosize metallic rod, a numerical simulation has been implemented to calculate the field distribution based on the finite difference method (FDM). The experimental and numerical results have been compared to show the suitability of EFM for the measurement of the local field at the surface of the nanotube arrays. Since there is a reciprocal screening in the nanotube thin film, the optimum combination of the extraction field and packing density of the nanotubes enable the maximum emission current. From our calculation, the geometrical parameters have been predicted for the highest electron emission efficiency.

II. EXPERIMENT

The anodic alumina has been fabricated by using the anodic alumina template method.[7] A layer of polycrystalline aluminum thin film has been deposited on the *n*-silicon wafer by vacuum evaporation. Using 0.3 M sulfate acid as an electrolyte, the aluminum thin films were anodized at the condition of 5 °C, 20 V, 1.5 h. Increasing the thickness of the aluminum thin film and anodizing time, the uniformity of the pore distribution can be improved.[8] After rinsing in 0.2 M phosphor acid for 60 min to thin the barrier layer at the bottom of the pores, the iron catalystic particles were electrodeposited to the bottom of the pores that were developed within alumina layer using saturate $FeSO_4$ aqueous solution with 20 V 50 Hz alternate drive voltage. Then the carbon

[a] Author to whom correspondence should be addressed; electronic mail: balong@seu.edu.cn

Downloaded 05 Apr 2011 to 158.132.161.9. Redistribution subject to AIP license or copyright; see http://jap.aip.org/about/rights_and_permissions

nanotubes were grown within pores by using C_2H_2, N_2, and H_2 mixture gases at a temperature of $680\pm10\,°C$ at the pressure of 200 mbar. The alumina layer was dissolved using 5% NaOH solution to expose the nanotubes. The morphologies of alumina films and nanotube arrays have been inspected by using a Digital Instrument IIIa atomic force microscope (AFM) and a scanning electron microscope (SEM).

In order to verify the electric contact between nanotubes and silicon wafer, we have measured the I–V response in the contact mode using a Seico SPI 3800N AFM. The test environment is 5×10^{-6} Torr. A SiliconMDT cantilever coated with WC and Au has been used. The force applied to the cantilever is about 280 nN. By pressing the cantilever to the end of various nanotubes, the I–V response has been recorded with both positive and negative biases.

The EFM images were taken in the tapping mode at a resonant frequency of 276.85 kHz for various lift heights. The topographic image and the EFM phase image were acquired simultaneously by scanning twice at the same line; one scan with the close loop control plots the topographic profile, while the next scan without the close loop control plots the phase or amplitude shift due to Columbic force by lifting the cantilever to various heights. A constant +1 V voltage has been applied to the cantilever while scanning at certain lift height. By measuring the amplitude or phase change of the fluctuation of the cantilever caused by Columbic force, the force gradient can be obtained from the formula: $\Delta A=(2A_0Q/3\sqrt{3}c)F'$,[9] where ΔA is the shift of amplitude induced by electric force and A_0, Q, c, and F' are the vibrating amplitude at resonance frequency, quality factor, elastic constant, and force gradient, respectively. The elastic constant c of the cantilever we used is about 1.4 N/m. Q factor of the cantilever used in experiment has been calibrated by fitting the Lorentzian equation:[9]

$$A(\omega)=\frac{A_0(\omega_0/\omega)}{\sqrt{1+Q^2(\omega/\omega_0-\omega_0/\omega)^2}}. \quad (1)$$

For all lift heights when bias was applied during experiment, the Q factor keeps constant around 60 ± 5.

The contrast of the amplitude image of EFM was transformed into the data of force gradient F'. Then the attractive electrostatic force on the EFM tip was obtained by integrating the F' curve from a series images with lift a height far from the sample surface to the height we concern. The nearest distance to the surface of the sample shall be larger than that above it the influence of the near surface force to the shift of phase is trivial. We started the lift height from 50 nm in the experiment. At this height, no contrast can be seen in the EFM image when no bias voltage has been applied. The amplitude of the free fluctuation of the cantilever is measured to be about 6 nm by calibrating the preamplifier of the AFM. This means that the fluctuation amplitude of the cantilever is far less than the lift height and the near surface force will not be involved in the EFM images.

Then, the strength of electric field can be calculated from electrostatic force $F=\frac{1}{2}VE_z^2\cdot S$, where V is the bias voltage applied between tip and sample, E_z is the vertical electric field strength at the end of the tip surface, and S is the effective area of tip (take it to be $2\pi r^2$, r is tip radius). Since the electric field strength obtained from the force gradient highly varies near sample surface, the effect of the base plate or trunk of the AFM tip to the electric field. In this way we have calculated the strength of electric field at the certain region of the sample.

III. NUMERICAL SIMULATION

The very simplified metallic cylinders standing on the metallic substrate were taken to resemble multiwall nanotube arrays in the following calculation. More detailed calculation for the field strength at the very vicinity of the tip of the nanotube requires the quantum treatment based on the local atomic positions. The dispersion of the local atomic structure and work function among a large number of nanotubes in the thin film causes the high fluctuation of electron emission among them. Since we mainly discuss the electric field at the distance several tens of nanometers away from the surface of the nanotube thin film, taking the nanotube as a metallic rod and using the traditional field calculation method are proper approximations for the calculation of the field induced by the AFM tip.

Being developed for decades, FDM has become a standard procedure for the field computation in recent years.[10] By using the Taylor formula, the potential at any point is transformed into the algorithm of neighboring points. The solution of the continuum Laplace equation is simplified into the solution of a series of linear equations with suitable boundary values by discrete the entire concerned region with grids of finite sizes. In order to make the calculation more efficient, the square grids have been applied to all concerned regions. The five-points Lagrange interpolation in the two-dimensional calculation has been used in the symmetry geometrical model. From boundary conditions, the potential of all nodes can be solved by iteration. The accuracy can be improved by designing finer grids and more layers. From the data of the earlier layer, the potential of the finer grids of the next layer can be calculated by a new set of iteration. We have designed 12 layers of grids. Figure 1(a) shows the illustration of the simplified geometry of the nanotubes and AFM tip. The AFM tip is modeled as a metallic cone covered by a partial spherical cap with a radius of 20 nm. On the same layer, finer grids were set to the regions where the field gradient is higher [Fig. 1(b)]. The metallic cylinder with a height of 375 nm and diameter of 20 nm is taken as a very simplified nanotube without consideration of hollow and doom structures.

IV. RESULTS AND DISCUSSIONS

Figure 2(a) and 2(b) are the AFM and SEM images of the anodic alumina surface and nanotube arrays, which show that the surface of the alumina within which the pores were developed is very flat within a single grain. From Fig. 2(b), it can be seen that the surface of the nanotube layer is almost the same height, and the side view shows that the fabric-like nanotubes grow perpendicular to the surface. By using this method, the diameter of the nanotube takes almost the same size as the pore of the anodic alumina and the roughness of

Downloaded 05 Apr 2011 to 158.132.161.9. Redistribution subject to AIP license or copyright; see http://jap.aip.org/about/rights_and_permissions

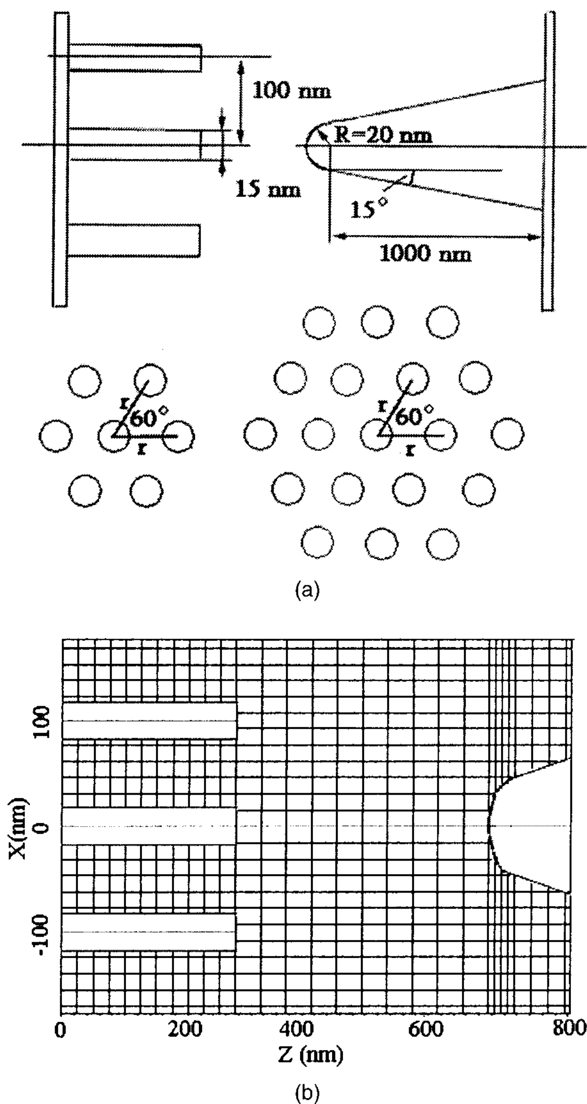

FIG. 1. Geometrical model (a) and example of grids (b) for electric field calculation.

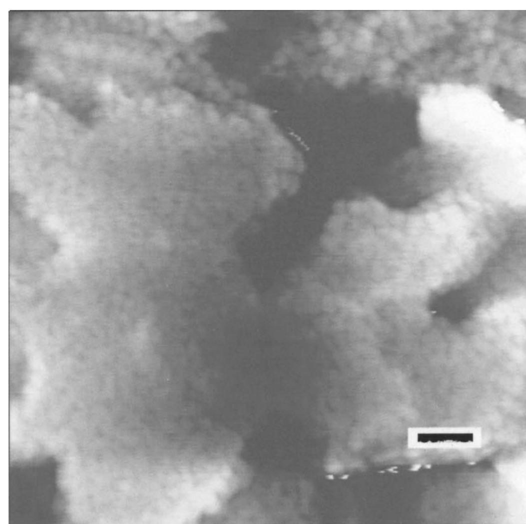

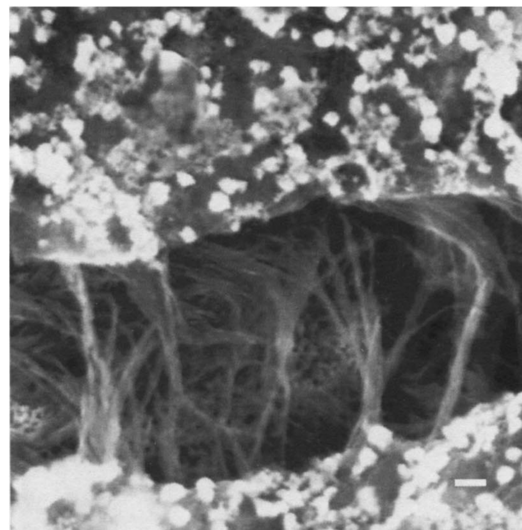

FIG. 2. AFM (a) and SEM (b) images of anodic alumina and nanotube thin films, scale is 100 nm.

the surface of the nanotube thin film inherits that of the aluminum film. The thickness of the nanotube thin film was measured to be 370–400 nm by checking the cross section of the nanotube layer using SEM, which is as thick as the alumina thin film.

Since the bottom of the pores within the alumina is opened by phosphor acid, and the alumina matrix shall be dissolved after growing nanotubes, there probably exists poor electronic contact between the nanotube, substrate, and chemical contaminants on the end of each nanotube. The poor contact will causes a high voltage drop and the possible breakdown at a higher applied bias. The chemical contaminants introduced by chemical vapor deposition and chemical treatment processes would cause an increase of the work function and the loss of electron emission efficiency. Through the conductive AFM experiment, we have verified the good electric contact between the nanotube and silicon substrate. By pressing the conductive AFM tip on the top of various nanotubes under the contact mode, three typical I–V curves have been measured and the results are plotted in Fig. 3. The results show that the resistance between the AFM tip and substrate at most locations is within the range of 10–300 kΩ. The surface contaminants such as the possible dielectric chemical debris is insulator and their sizes in most cases are less or close to the diameter of the nanotubes. Thus, it is reasonable to think that their shielding effect to the field at the ends of the nanotubes is minor.

Figures 4(a), 4(b), and 4(c) show the AFM image [Fig. 4(a)], EFM phase images with lift heights of 50 nm [Fig. 4(b)] and 200 nm [Fig. 4(c)] for a typical region of the nanotube arrays after dissolving the alumina matrix. The contrast of the EFM image is the shift of the vibration phase, which is proportional to the differential force along the vertical direction. From EFM phase images, the amplitude changes can be calculated, thus the force gradients at each lift height were calculated. Figure 5 shows the force gradients, electrostatic forces, and the corresponding strengths of the electric field at

Downloaded 05 Apr 2011 to 158.132.161.9. Redistribution subject to AIP license or copyright; see http://jap.aip.org/about/rights_and_permissions

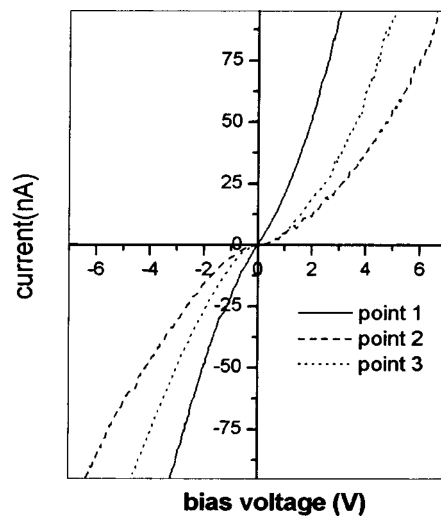

FIG. 3. I–V curves measured by using the conductive AFM tip.

various lift heights (L) of two nanotubes as indicated in Fig. 4. By fitting the log–log plots of the force gradients, the linear relation of $\log(F')$ vs $\log(L)$ means that the F' is proportional to the exponential of L, which is similar to that observed for the conical field emitter of submicrometer .[6]

The parameters used in the calculation are close to that of the nanotubes arrays fabricated as described earlier. The anode voltage is 1 V and the cathode is grounded. The height of the nanotube is 375 nm and the diameter of the nanotube is 20 nm. The tip is placed at various heights (L: 50–400 nm) right above the nanotube of the center one to calculate the field at these positions. The field has also been calculated with a planar anode. The distance from the AFM tip to the end of the nanotube is 100 nm. In order to see the field enhancement of the nanotube arrays of various packing densities, the distance between the neighboring nanotubes is set from tens to hundreds of nanometers. Based on these parameters, we have calculated the potential and field strength for 1, 7, and 19 nanotubes [7 and 19 nanotubes are hexagonally aligned as shown in the inset of Fig. 1(a)]. Figure 6(a) shows the potential distribution between the AFM tip and nanotubes. Thus, the 3D field distribution can be calculated from the numerical results of potential. The E_z at various positions with the planar anode/nanotube cathode and AFM tip anode/nanotube cathode has been plotted in Fig. 6(b). The field sensed by the AFM tip has been calculated to simulate the experiment results. Both results are plotted in Fig. 7.

From earlier results, the growth of the nanotubes is confined by pores within the anodic alumina template, the diameters of all nanotubes scatter within a very narrow region and the heights of the nanotubes are also almost the same. The fluctuation of the field enhancement induced by the dispersion of the height and diameter is minimal compared to the nanotube arrays fabricated using other methods. From Fig. 3, the I–V response is symmetrical under the positive and nega-

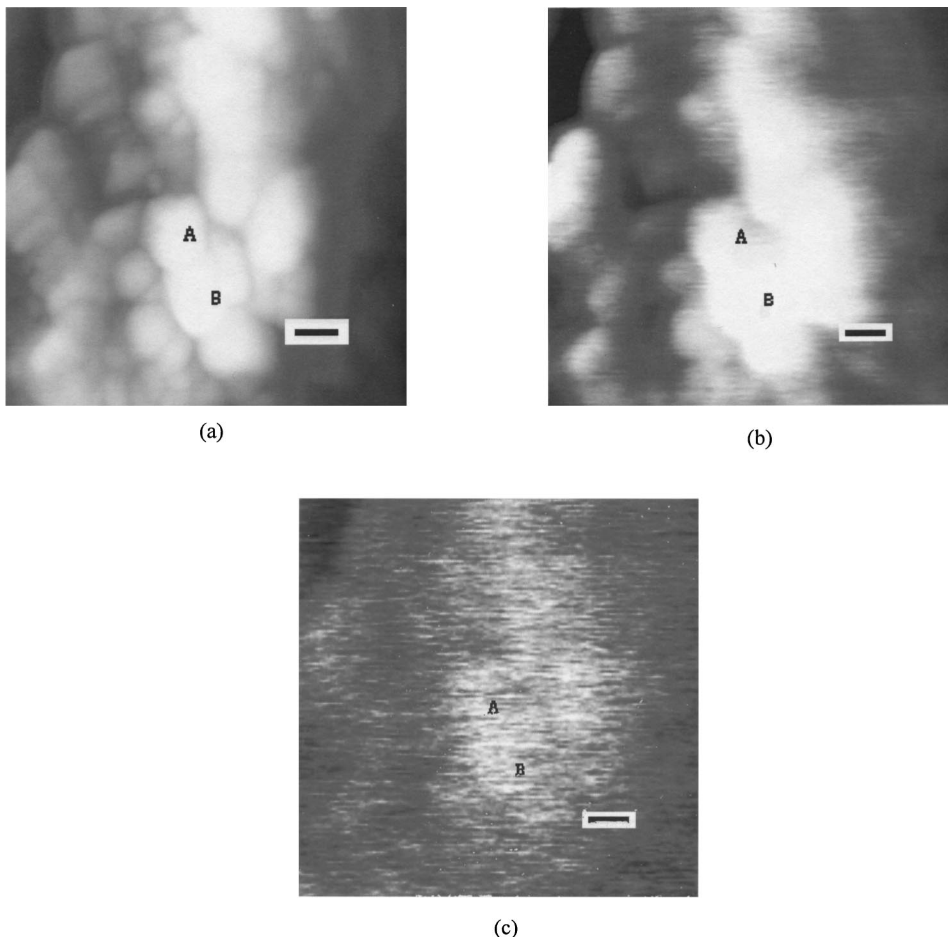

FIG. 4. Topographic and EFM phase images of nanotube arrays, (a) tapping mode AFM image, (b) EFM phase image with a lift height of 50 nm, and (c) EFM image with a lift height of 300 nm, scale is 100 nm.

Downloaded 05 Apr 2011 to 158.132.161.9. Redistribution subject to AIP license or copyright; see http://jap.aip.org/about/rights_and_permissions

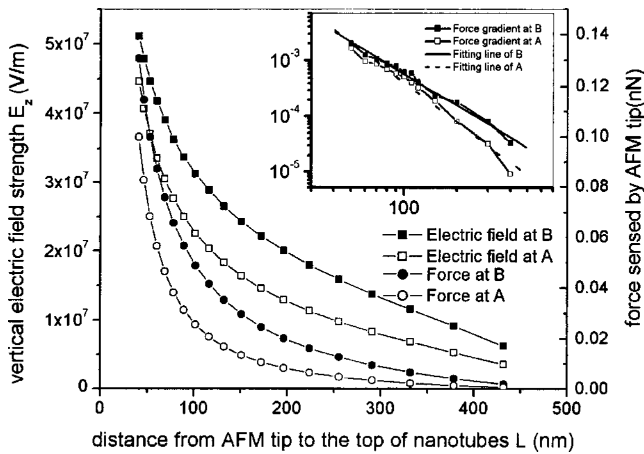

FIG. 5. Electrostatic force and electric field obtained from measured results. The inset is the log–log plots of force gradients at various lift heights and the linear fitting lines.

tive bias. This response does not change much when the force applied to the cantilever is increased or decreased several tens of nanonewtons. Though two types of I–V response can be found (ohmic and tunneling), most nanotubes have a linear current response at higher bias voltages and symmetry I–V response can be observed for every nanotube. This means that the series resistance of the AFM tip/nanotube/substrate in most cases is ohmic. Since the contaminants at the surface of nanotube thin film is less significant, the tunneling like I–V response observed in a few points might be mainly induced by the weak contact between the nanotube and silicon substrate.

Figure 6(b) shows that the electrostatic screening effect introduced by the proximity of the vertically packed tubes will be diminished when the space between the neighboring nanotubes exceeds 450 nm. This distance is less than that predicted by Nilsson,[11] which is about two times of the height of the nanotube. The discrepancy may be caused by the difference of nanotube packing geometry (hexagonal packed nanotubes in our model). From the Fowler–Nordheim equation: $j \propto (E_{\mathrm{loc}}^2/\Phi)\exp(-6.8\times 10^9 \Phi^{3/2}/E_{\mathrm{loc}})$ (j is the emission current, Φ is the work function, and E_{loc} is the effective local field strength), the maximum emission current is the combination of the extraction field and packing density. The emission current can be calculated for various packing densities [Fig. 6(c)]. The maximum collective emission happens at a medium packing density.

From Fig. 7, it can be seen that the experimental results are close to the numerical data at the region near the sample surface, but the experimental results decay faster than all the numerical data. At the far region, there are some discrepancies. These discrepancies shall be mainly created by the less integrating points in the discrete integration of F' at the higher tip/sample space end and the weak sensitivity of the cantilever to the field at the distance L higher than 500 nm.

The accuracy of the measured E_z could be further improved by recording more F' at various lift heights and using more accurately calibrated cantilever parameters. Using a much softer cantilever will increase the signal/noise ratio. The near surface force gradient can be acquired by subtracting the contrast of the images after and before the bias is applied. From fitting the linear section (<150 nm) of all five plots in Fig. 7, the field strength can be expressed as E–L^{-c}, where z is the distance from the tip to the top of the nano-

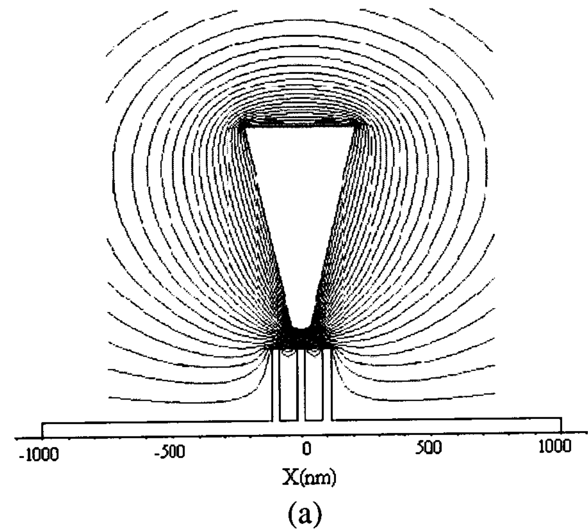

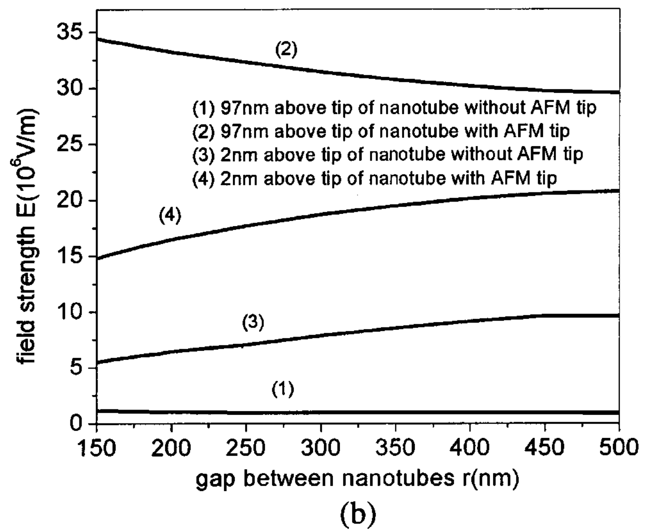

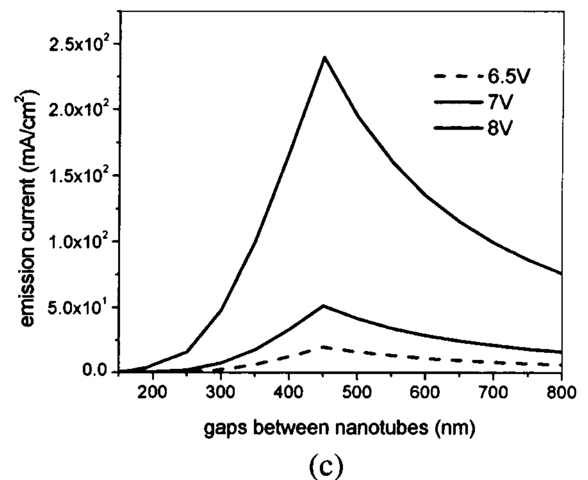

FIG. 6. Equipotential lines of the electric field between AFM tip and nanotube arrays (a), electric field strength for various gaps between the nanotubes with a planar anode and AFM tip anode (b), and emission current for various gaps between nanotubes (c).

Downloaded 05 Apr 2011 to 158.132.161.9. Redistribution subject to AIP license or copyright; see http://jap.aip.org/about/rights_and_permissions

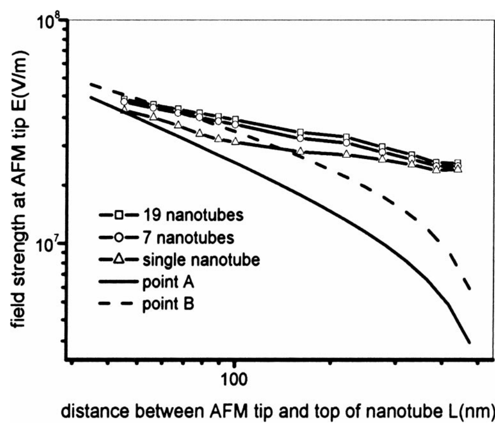

FIG. 7. Log–log plots of measured (lines with symbols) and calculated (thick solid line and dash line) electric field with various lift heights of the AFM tip.

tubes and c varies from 0.536 (location B) to 0.742 (location A). The exponent obtained from the numerical results of 1, 7, 19 nanotube array is 0.518, 0.421, and 0.378, respectively. It shows that the field decays much faster than that of the numerical results. The numerical results also exponentially decay as the AFM tip is moved away from the nanotubes. The decay exponent for a single nanotube is higher than that for more nanotubes, which is consistent with the fact that the single nanotube produces the highest field enhancement. Comparing the experimental plots A and B, the field above the more protruding nanotube (B) decay slower than that above the lower nanotube (A). This apparent inconsistency with the result of calculation might be induced by the variation of the local stray field, since the nanotubes of the experimental sample are not very uniform in both the packing position and height. The experimental plots in Fig. 7 show that the enhanced field is higher for the nanotube with more protrusion, while the calculation shows the field for a single tube is less than that induced by more tubes at a lift height of 50 nm. This means that the stay field at the location several tens of a nanometer away from the end of the tubes excesses the field enhanced by a sharp curvature of cathode at this location.

From Fig. 6(b), it can be seen that the local field is heavily convoluted by the AFM tip. It is interesting to see that the fields near the end of the nanotubes as the anode vary in a similar tendency with or without the AFM tip while the gap between the neighboring tubes increases. This field enhanced by both the nanotubes and AFM tip. Although the convolution of the AFM tip to the field enhancement will cause more discrepancies than planar or other shape anodes, the field measured can display the influence of cathode geometry to the local field distribution with increased sensitivity.

V. CONCLUSIONS

The above experimental study demonstrates that the local electric field near the ending surface of the nanotube arrays can be measured using EFM technology by recording a series of force gradient signals over the same region. The numerical calculation shows that the local field is enhanced by the AFM tip, which exhibits a similar variation tendency as the planar anode for different packing densities. The experiment and numerical results at the AFM tip show that the field strength decays in a power low with various exponents while lifting the tip away from surface of the nanotube thin film. For the case of that the diameter diversity of the nanotubes is trivial, the height scattering and assembled density of the nanotubes mostly affect the uniformity of the electric field near the cathode surface.

ACKNOWLEDGMENTS

This project is supported by Natural Science Foundation of China (60121101) and Southeast University of China internal new faculty Grant No. (9207031138). The authors would like to thank X. P. Wang of the University of Science and Technology of China for help with the vacuum AFM test and C. X. Xu and N. Y. He of Southeast University of China for help with the sample preparation.

[1] P. G. Collins and A. Zettl, Appl. Phys. Lett. **69**, 1969 (1996).
[2] Y. Saito *et al.*, Appl. Phys. A: Mater. Sci. Process. **67**, 95 (1998).
[3] O. Groning, O. Kuttel, C. Emmenegger, P. Groning, and L. Schlapbach, J. Vac. Sci. Technol. B **18**, 665 (2000).
[4] R. Gao, Z. Pan, and Z. L. Wang, Appl. Phys. Lett. **78**, 1757 (2001).
[5] Y. Saito and S. Uemura, Carbon **38**, 169 (2000).
[6] Y. Liang, D. A. Bonnell, W. D. Goodhue, D. D. Rathman, and C. O. Bozler, Appl. Phys. Lett. **66**, 1147 (1995).
[7] J. Li, C. Papadopoulos, J. M. Xu, and M. Moskovits, Appl. Phys. Lett. **75**, 367 (1999).
[8] L. Ba and W. S. Li, J. Phys. D **33**, 2527 (2001).
[9] Y. Matin, D. Rugar, H. R. Hidber, and H. J. Guntherodt, J. Appl. Phys. **61**, 4723 (1987).
[10] P. W. Hawkes and E. Kasper, *Principles of Electron Optics* (Academic, New York, 1996), Vol. 1.
[11] L. Nisson *et al.*, Appl. Phys. Lett. **76**, 2071 (2000).

Downloaded 05 Apr 2011 to 158.132.161.9. Redistribution subject to AIP license or copyright; see http://jap.aip.org/about/rights_and_permissions